SAGE-Hindawi Access to Research
International Journal of Alzheimer's Disease
Volume 2011, Article ID 925073, 8 pages
doi:10.4061/2011/925073

Research Article

Spectroscopic Characterization of Intermolecular Interaction of Amyloid β Promoted on GM1 Micelles

Maho Yagi-Utsumi,[1,2] Koichi Matsuo,[3] Katsuhiko Yanagisawa,[4] Kunihiko Gekko,[3] and Koichi Kato[1,2]

[1] *Graduate school of Pharmaceutical Sciences, Nagoya City University, 3-1 Tanabe-dori, Mizuho-ku, Nagoya 467-8603, Japan*
[2] *Institute for Molecular Science and Okazaki Institute for Integrative Bioscience, National Institutes of Natural Sciences, 5-1 Higashiyama, Myodaiji, Okazaki 444-8787, Japan*
[3] *Hiroshima Synchrotron Radiation Center, Hiroshima University, 2-313 Kagamiyama, Higashi-Hiroshima 739-0046, Japan*
[4] *Department of Alzheimer's Disease Research, National Center for Geriatrics and Gerontology, National Institute for Longevity Sciences, 36-3 Gengo, Morioka, Obu, Aichi 474-8522, Japan*

Correspondence should be addressed to Koichi Kato, kkatonmr@ims.ac.jp

Received 13 October 2010; Revised 30 November 2010; Accepted 3 December 2010

Academic Editor: J. Fantini

Clusters of GM1 gangliosides act as platforms for conformational transition of monomeric, unstructured amyloid β (Aβ) to its toxic β-structured aggregates. We have previously shown that Aβ(1–40) accommodated on the hydrophobic/hydrophilic interface of lyso-GM1 or GM1 micelles assumes α-helical structures under ganglioside-excess conditions. For better understanding of the mechanisms underlying the α-to-β conformational transition of Aβ on GM1 clusters, we performed spectroscopic characterization of Aβ(1–40) titrated with GM1. It was revealed that the thioflavin T- (ThT-) reactive β-structure is more populated in Aβ(1–40) under conditions where the Aβ(1–40) density on GM1 micelles is high. Under this circumstance, the C-terminal hydrophobic anchor Val^{39}-Val^{40} shows two distinct conformational states that are reactive with ThT, while such Aβ species were not generated by smaller lyso-GM1 micelles. These findings suggest that GM1 clusters promote specific Aβ-Aβ interactions through their C-termini coupled with formation of the ThT-reactive β-structure depending on sizes and curvatures of the clusters.

1. Introduction

Conformational transitions of unstructured proteins into β-structure-based oligomeric or amyloid states are crucial processes in the onset and development of a variety of neurodegenerative disorders such as Alzheimer's disease (AD) and Parkinson's disease [1, 2]. Amyloid β(Aβ), a major player in AD, is a 40- or 42-amino acid peptide cleaved from its precursor membrane protein by sequential actions of β- and γ-secretases and has a high propensity for toxic aggregation to form cross-β-fibrils [3, 4]. Accumulated evidence indicates that the GM1 ganglioside, a glycosphingolipid abundant in neuronal cell membranes, interacts with Aβ and promotes its assembly, resulting in pathogenic amyloid formation [5–7]. For example, high-density GM1 clustering, which is exclusively observed in synaptosomes, is suggested to accelerate Aβ deposition [8]. *In vitro* experiments have indicated that the Aβ-GM1 interaction depends on the clustering of GM1, and its carbohydrate moiety alone cannot induce conformational changes of Aβ [15, 30, 31].

Furthermore, it has been suggested that each of the heredity variants of Aβ reported thus far has its own specificities for gangliosides, which have been supposed to be associated with their ectopic deposition [9, 10]. Promotion of amyloid formation in membrane-bound states has also been reported for prion and α-synuclein [11, 12]. For example, prion protein has been reported to be localized in the membrane microdomains and caveolae enriched with ganglioside, which interacts with prion protein and thereby promotes its α-to-β structural conversion [13, 14]. Therefore, detailed conformational characterization of Aβ interacting with the ganglioside clusters not only provides

structural information as cues for drug development in preventing and treating AD but also offers general insights into the mechanisms underlying the disease-associated amyloid formation facilitated in membrane environments.

In previous papers, we have reported nuclear magnetic resonance (NMR) studies of the interactions of Aβ (1–40) with ganglioside clusters using lyso-GM1 micelles (approximate molecular mass 60 kDa) as model systems [15, 16]. Our NMR data showed that Aβ(1–40) is accommodated on the hydrophobic/hydrophilic interface of the ganglioside cluster exhibiting an α-helical conformation under ganglioside-excess conditions. In this state, Aβ(1–40) shows an up-and-down topological mode in which the two α-helices at segments His^{14}-Val^{24} and Ile^{31}-Val^{36} and the C-terminal Val^{39}-Val^{40} dipeptide segment are in contact with the hydrophobic interior of the micelles, whereas the remaining regions are exposed to the aqueous environment. A similar tendency of Aβ(1–40) has been observed using excess amounts of GM1, which forms micelles with an approximate molecular mass of 140 kDa [15, 17]. These findings indicate that ganglioside clusters offer unique platforms at their hydrophobic/hydrophilic interfaces for binding coupled with α-helix formation of Aβ molecules.

To gain further insights into the underlying mechanisms of the amyloid formation of Aβ, it is necessary to characterize the conformational transition from α-helices to β-structures on the ganglioside clusters. On the basis of the circular dichroism (CD) data, Kakio et al. demonstrated that Aβ/GM1 ratios influence the secondary structure of Aβ(1–40) on the raft-like lipid bilayers composed of GM1, cholesterol, and sphingomyelin [18, 19]. Namely, Aβ adopts an α-helical structure at lower Aβ/GM1 ratios ($\leq$0.025), while it assumes a β-sheet-rich structure at higher ratios ($\geq$0.05). Although more detailed structural information on Aβ bound to the GM1 cluster is highly desirable, the small unilamellar vesicles used for the CD measurements are still too large to investigate with solution NMR techniques.

In the present study, we attempt to characterize conformational states of Aβ(1–40) in the presence of varying amounts of GM1 aqueous micelles using stable-isotope-assisted NMR spectroscopy in conjunction with synchrotron-radiation vacuum-ultraviolet CD (VUVCD) spectroscopy. We found that GM1 micelles also induce distinct secondary structures of Aβ(1–40) depending on the Aβ/GM1 ratios. On the basis of the spectroscopic data, we will discuss Aβ behaviours on the ganglioside clusters from a structural point of view.

2. Materials and Methods

2.1. Preparation of Aβ(1–40). Recombinant Aβ(1–40) was expressed and purified as a ubiquitin extension. The plasmid vector encoding Aβ(1–40) was constructed and cloned as a fusion protein with hexahistidine-tagged ubiquitin (His_6-Ub) using the pET28a(+) vector (Novagene), subsequently transformed into *Escherichia coli* strain BL21-CodonPlus (Stratagene) [15]. Transformed bacteria were grown at 37°C in LB media containing 15 μg/mL of kanamycin. For the production of isotopically labelled Aβ(1–40) protein, cells were grown in M9 minimal media containing [^{15}N] NH_4Cl (1 g/L) and/or [U-$^{13}C_6$] glucose (2 g/L). Protein expression was induced by adding 0.5 mM isopropyl-β-$_D$-thiogalactopyranoside (IPTG) when the absorbance reached 0.8 at 600 nm. After 4 hours, cells were harvested and then suspended into buffer A (50 mM Tris-HCl, 150 mM NaCl, pH 8.0) containing 4-(2-aminoethyl) benzenesulfonyl fluoride hydrochloride, subsequently disrupted by sonication. After centrifugation, the pellet was dissolved in buffer A containing 8 M urea. His_6-Ub-Aβ(1–40) was purified by a Ni^{2+}-nitrilotriacetic acid affinity column (GE Healthcare). Recombinant glutathione *S*-transferase- (GST-) tagged yeast ubiquitin hydrolase-1 (YUH-1) was grown until the absorbance reached 0.8 at 600 nm and then induced to express by IPTG. Cell pellets were dissolved in buffer B (50 mM Tris-HCl, 1 mM EDTA, 1 mM DTT, pH 8.5) and disrupted by sonication. GST-YUH-1 was purified by a glutathione affinity column (GE Healthcare). Aβ(1–40) protein was enzymatically cleaved from His_6-Ub by incubation with GST-YUH-1 for 1 h at 37°C at a molar ratio of His_6-Ub-Aβ(1–40): GST-YUH1 = 10 : 1. The cleaved Aβ(1–40) was purified by reverse-phase chromatography using an octadecylsilane column (TSKgel ODS-80T_M, TOSOH) with a linear gradient of acetonitrile. The fraction containing Aβ(1–40) was collected and lyophilized.

Synthetic Aβ(1–40) labelled with ^{15}N selectively at Val^{39} or Val^{40} was purchased from AnyGen Co. Both of recombinant and synthetic Aβ(1–40) proteins were dissolved at an approximate concentration of 2 mM in 0.1% (v/v) ammonia solution then collected and stored in aliquots at −80°C until use.

2.2. Preparation of Micelles. Powdered lyso-GM1 and GM1 were purchased from Takara Bio Inc. and Sigma-Aldrich, respectively. These gangliosides were dissolved in methanol. Subsequently, the solvent was removed by evaporation. The residual ganglioside was suspended at a concentration of 12 mM in 10 mM potassium phosphate buffer (pH 7.2) and then mixed by vortexing. Micelle sizes were determined by dynamic light scattering using a DynaPro Titan (Wyatt technology).

2.3. Thioflavin T (ThT) Assay. Aβ(1–40) was dissolved at a concentration of 0.2 mM in 10 mM potassium phosphate buffer (pH 7.2) in the absence or presence of 0.4–9 mM GM1 or lyso-GM1. The samples were kept on ice before measurements. 980 μL of 5 μM ThT (Sigma) solution in 50 mM glycine-NaOH buffer (pH 8.5) was added to an aliquot of 20 μL of each sample. Fluorescence was measured immediately after mixing at the excitation and emission wavelengths of 446 and 490 nm, respectively, [20] using spectrofluorophotometer (Hitachi F-4500) at 37°C.

2.4. VUVCD Measurements. Aβ(1–40) was dissolved at a concentration of 0.2 mM in 10 mM potassium phosphate buffer (pH 7.2). The CD spectra of Aβ(1–40) in the presence or absence of GM1 were measured from 265 to 175 nm under a high vacuum (10^{-4} Pa) at 37°C using the VUVCD spectrophotometer constructed at beamline

15 (0.7 GeV) of the Hiroshima Synchrotron Radiation Center (HiSOR). Details of the spectrophotometer and optical cell were described previously [21, 22]. The path length of the CaF_2 cell was adjusted with a Teflon spacer to 50 μm or 100 μm for measurements. The VUVCD spectra were recorded with a 1.0-mm slit, a 16-s time constant, a 4-nm min^{-1} scan speed, and nine accumulations. The molar ellipticities of Aβ(1–40) were calculated with the average residue weight of 107.5. The secondary structure contents of Aβ(1–40) were analysed using the modified SELCON3 program [23] and the VUVCD spectra down to 160 nm for 31 reference proteins with known X-ray structures [24, 25]. The secondary structures of these proteins in crystal form were assigned into four classes (α-helices, β-strandes, turns, and unordered structures) using the DSSP program [26] based on the hydrogen bonds between adjacent amide groups. In this analysis, the 3_{10}-helix was classified as an unordered structure. The root-mean-square deviation (δ) and the Pearson correlation coefficient (r) between the X-ray and VUVCD estimates of the secondary structure contents of the reference proteins were 0.058 and 0.85, respectively, confirming the high accuracy of the VUVCD estimation [27].

2.5. NMR Measurements. NMR spectral measurements were made on a Bruker DMX-500 spectrometer equipped with a cryogenic probe as well as a Bruker AVANCE III-400 spectrometer. The probe temperature was set to 37°C. Isotopically labelled Aβ(1–40) was dissolved at a concentration of 0.2 mM in 10 mM potassium phosphate buffer (pH 7.2) containing 10% (v/v) ^2H_2O in the presence or absence of GM1. For ^1H-^{15}N heteronuclear single-quantum correlation (HSQC) measurements, the spectra were recorded using Aβ(1–40) labelled with ^{15}N uniformly or selectively at the amide group of Val^{39} or Val^{40} at a ^1H observation frequency of 500 MHz with 128 (t_1) × 1024 (t_2) complex points and 256 scans per t_1 increment. The spectral width was 1720 Hz for the ^{15}N dimension and 6000 Hz for the ^1H dimension.

One-dimensional carbonyl ^{13}C spectra were recorded using uniformly ^{13}C- and ^{15}N-labelled Aβ(1–40) at a ^1H observation frequency of 400 MHz with a spectral width of 22,000 Hz. In these experiments, 32,768 data points for acquisition and 16,384 scans were acquired. NMR spectra were processed and analysed with the program nmrPipe/Sparky.

3. Results

3.1. ThT Fluorescence Enhancement. We examined whether ThT fluorescence is enhanced by Aβ(1–40) in the presence of varying concentrations of GM1 or lyso-GM1. As shown in Figure 1, GM1 exhibited a bell-shaped dependence on Aβ/GM1 ratios regarding ThT fluorescence enhancement, while lyso-GM1 showed virtually no enhancement. Maximum enhancement was observed at a 1:15 molar ratio of Aβ(1–40) to GM1. The dynamic light scattering data confirmed that the GM1 and lyso-GM1 micelles exhibited an approximate hydrodynamic radius of 6 nm and 4 nm, respectively, irrespective of the Aβ/ganglioside ratios. The

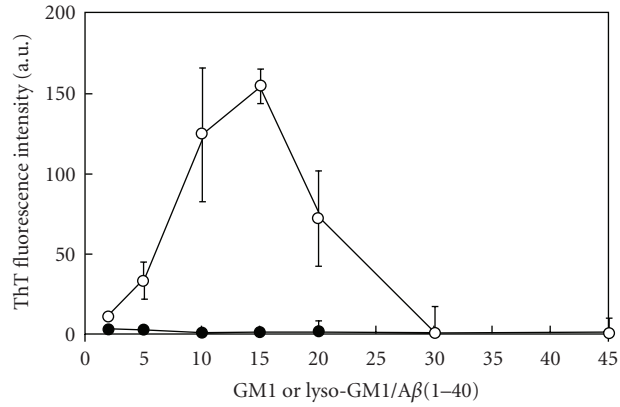

Figure 1: ThT fluorescence enhancement by Aβ(1–40) in the presence of varying concentrations of GM1 (open circle) or lyso-GM1 (closed circle). Each intensity value indicates the average of four values ± S.D.

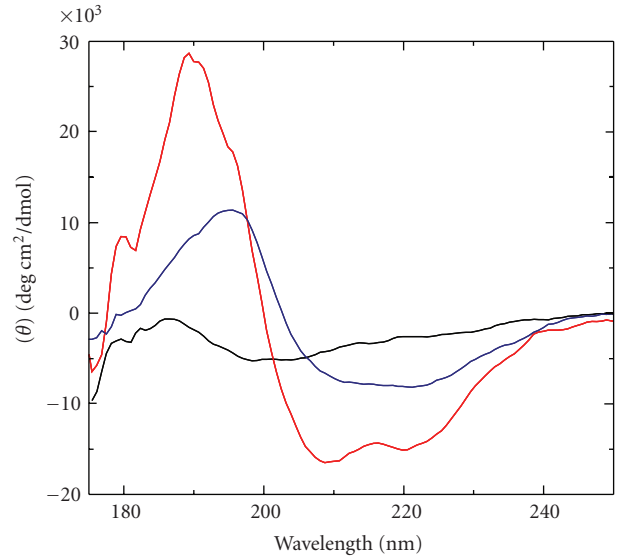

Figure 2: VUVCD spectra of 0.2 mM Aβ(1–40) in the absence or presence of GM1. Aβ/GM1 molar ratios were 1 : 0 (black), 1 : 15 (blue), and 1 : 30 (red).

observed fluorescence intensity remained almost constant up to 12 h. These data indicated that GM1 micelles at appropriate Aβ/GM1 ratios promote some Aβ–Aβ interaction with formation of their β-sheet-like conformation, which, however, does not result in irreversible fibril formation.

3.2. Secondary Structure Transition. We characterized the conformational transition of Aβ depending on Aβ/GM1 ratios by CD measurements. The short-wavelength limit of CD spectroscopy can be successfully extended using synchrotron radiation as a high-flux source of photons, which yields much more accurate data than those obtained with a conventional CD spectrophotometer [28, 29]. The spectral data indicated that Aβ(1–40) undergoes conformational transitions depending on GM1 to Aβ(1–40) ratios (Figure 2).

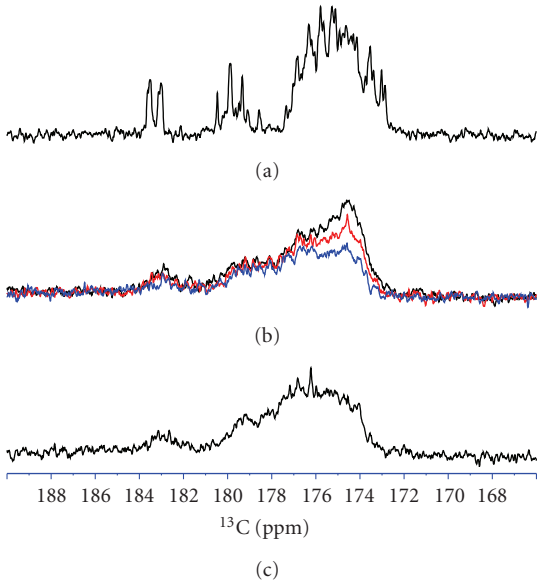

Figure 3: Carbonyl ^{13}C spectra of uniformly ^{13}C-labelled Aβ(1–40). Spectral data were obtained using 0.2 mM Aβ(1–40) titrated with GM1 micelles at Aβ/GM1 molar ratios of (a) 1 : 0, (b) 1 : 15, and (c) 1 : 30. In (b), the spectra measured in the presence of ThT are displayed at Aβ/ThT molar ratios of 1 : 0 (black), 1 : 1 (red), and 1 : 2 (blue).

Table 1: Secondary structure contents (%) of Aβ(1–40) from VUVCD spectra obtained in the presence of varying concentrations of GM1.

Aβ : GM1	α-Helix	β-Strand	Turn	Unordered structure
1 : 0	15.9	17.8	26.3	39.0
1 : 15	23.6	23.6	21.6	29.3
1 : 30	40.0	18.3	14.5	27.9

The secondary structure contents of Aβ(1–40) at Aβ/GM1 molar ratios of 1 : 0, 1 : 15, and 1 : 30 were estimated on the basis of the spectral data (Table 1). The α-helix content of Aβ(1–40) in the presence of GM1 at an Aβ/GM1 molar ratio of 1:30 was calculated to be 40.0%, which is consistent with our previous estimation based on the backbone chemical shift data of lyso-GM1 [15], thus confirming close similarity of the binding modes of Aβ(1–40) between GM1 and lyso-GM1micelles. At an Aβ/GM1 molar ratio of 1:15, where the maximum ThT fluorescence enhancement was observed, the CD data consistently indicated a significantly increased content of β-strands.

The conformation of Aβ(1–40) in the presence of varying amounts of GM1 micelles was further characterized by ^{13}C NMR spectroscopy. The carbonyl ^{13}C NMR spectral data of uniformly ^{13}C-labelled Aβ(1–40) indicated that the peaks shifted upfield, roughly corresponding to β-structures, are more populated at an Aβ/GM1 molar ration of 1 : 15 in comparison with the GM1-excess conditions (Figure 3). Intriguingly, intensities of these peaks were selectively reduced upon the addition of ThT. These NMR data are again consistent with the VUVCD data as well as the results of the ThT assay.

3.3. Local Structure of the C-Terminus of Aβ(1–40). To provide more detailed information on the conformational transition of Aβ(1–40) on GM1 micelles, we observed ^{1}H-^{15}N HSQC spectral changes of Aβ(1–40) upon titration with GM1. Interestingly, at an Aβ/GM1 molar ratio of 1 : 15, Aβ(1–40) exhibited HSQC peaks that were not observed in the spectra of free or fully micelle-bound forms (Supplementary Figure 1). By using site-specifically ^{15}N-labelled Aβ, these extra peaks were assigned to Val^{39} and Val^{40} (Figure 4 and Supplementary Figure 1 available online at doi:10.4061/2011/925073). Namely, the amide groups of these C-terminal residues of the micelle-bound Aβ species show double HSQC peaks under the condition where Aβ/GM1 ratio is relatively high. More interestingly, these double peaks were perturbed upon the addition of ThT, while the corresponding peaks originating from the free and fully micelle-bound forms showed little or no change (Figure 4). On the other hand, many of the ^{1}H-^{15}N HSQC peaks from Aβ(1–40), including Val^{39} and Val^{40}, were not observed at an Aβ/lyso-GM1 molar ratio of 1 : 15 due to intermediate chemical exchange between free and micelle-bound states of Aβ(1–40) (data not shown).

4. Discussion

Accumulating evidence, including our previous reports, indicates that the interaction of Aβ with GM1 involves multiple steps including the initial encounter complex formation and the accommodating process on the hydrophilic/hydrophobic interface of the ganglioside clusters [15–17, 30]. NMR spectral data of Aβ(1–40) titrated with GM1 micelles under Aβ-excess conditions indicated that they form a weak complex presumably through an interaction between the N-terminal segment of Aβ(1–40) and the outer carbohydrate branch of GM1 [15, 30]. Thus, it is conceivable that the outer-branch structures of the carbohydrate moieties of gangliosides influence the association phase of the interaction and thereby determine the ganglioside specificities of Aβ. Nongangliosidic micelles and vesicles are barely or not capable of trapping Aβ(1–40) effectively [15, 18, 31, 32]. On the other hand, the α-helical conformation of Aβ(1–40) accommodated on sugar-lipid interface of the GM1 and lyso-GM1 micelles have been characterized by NMR under ganglioside-excess conditions (Aβ/ganglioside molar ratio of 1 : 30) [15]. Because the structure of the inner part is common among the gangliosides, non-GM1 ganglioside, for example, GM2, can accommodate Aβ and induce its α-helical conformation [16]. Thus, the spectroscopic characterization of the interactions of Aβ with gangliosidic micelles has so far been performed only under the extreme conditions of the Aβ/ganglioside ratios. The present study attempts to bridge the gap in our understanding of Aβ behavior on GM1 micelles by carrying out spectroscopic analyses of Aβ in the presence of varying amounts of GM1 micelles.

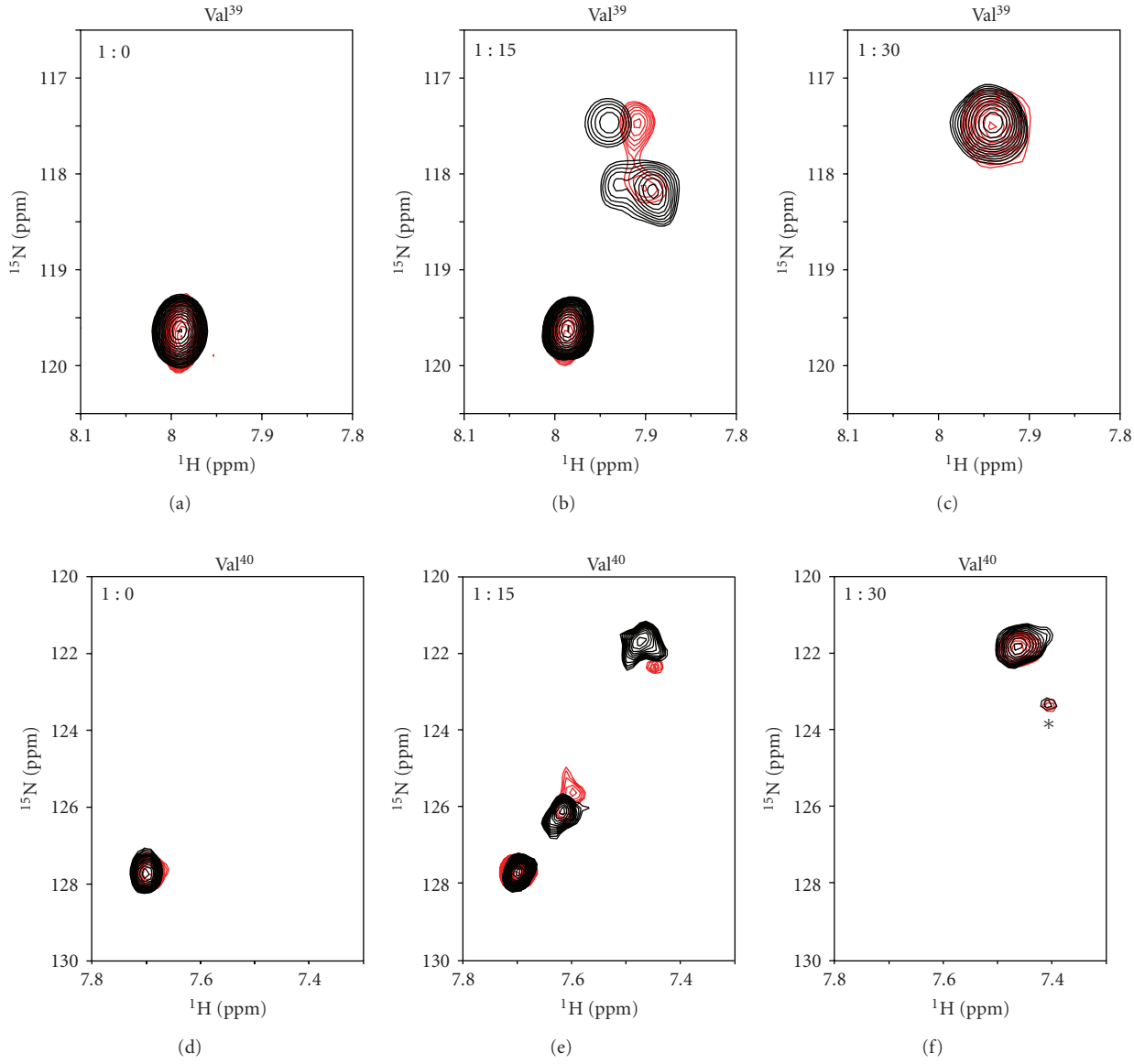

Figure 4: ^{1}H-^{15}N HSQC peak originating from Val^{39} (upper) and Val^{40} (lower) of Aβ(1–40) in the presence or absence of GM1 micelles and ThT. Site specifically ^{15}N-labelled Aβ(1–40) proteins (0.2 mM each) were titrated with GM1 at Aβ/GM1 molar ratios of 1 : 0 (a, d), 1 : 15 (b, e), and 1 : 30 (c, f). The spectra measured in the absence (black) and presence (red) of 0.4 mM ThT are overlaid. The peak indicated by asterisk originated from GM1.

The present data all indicated that β-structure is more populated in micelle-bound Aβ(1–40) under the condition where the Aβ/GM1 ratio is higher. It is intriguing that the increased β-structure is reactive with ThT. Although the binding mode of ThT to amyloid fibrils has yet to be fully elucidated, it has been suggested that ThT is more likely to bind perpendicularly to parallel β-strands in a β-sheet [33–35]. In addition, recently reported solid-state NMR data indicate that a ThT-reactive, neurotoxic amyloid intermediate of Aβ(1–40) is composed of parallel β-structures [36]. These data suggest that formation of parallel β-strands is the minimum prerequisite for ThT fluorescence enhancement. With this in mind, the bell-shape dependence of ThT fluorescence enhancement (Figure 1) can be interpreted as follows. At an extremely low concentration of GM1, most of Aβ(1–40) exists as a free form, which is an unstructured monomer and therefore is not reactive with ThT. Fraction of the micelle-bound form of Aβ(1–40) increases with increase of the GM1 amounts. To some extent, the micelles promote intermolecular interaction of Aβ(1–40), giving rise to the ThT-reactive Aβ(1–40) species. Under GM1-excess conditions, however, Aβ(1–40) molecules are presumably relatively isolated from one another and therefore are not capable of forming an intermolecular β-structure. The Aβ/GM1 molar ratio, where the maximum enhancement was observed, was 1 : 15, which corresponds to average number of Aβ/micelle of 11.2 with the assumption of the micellar GM1 aggregation number of 168 ± 4 [37]. Thus, the Aβ density on

GM1 micelles is a crucial factor determining the occurrence of the ThT-reactive Aβ species.

Under the circumstance where the Aβ(1-40) density on GM1 micelles is high, the C-terminal dipeptide of Aβ(1–40) shows, at least, two distinct conformational states that are reactive with ThT. In a previous paper, we demonstrated that the C-terminal Val^{39}-Val^{40} dipeptide is inserted into the hydrophobic interior of the gangliosidic micelles [15]. This C-terminal segment is involved in the parallel β-structure in the amyloid fibril and intermediate [36, 38]. On the basis of these data, we suggest that GM1 clusters promote intermolecular Aβ-Aβ interactions coupled with the conformational transition of their C-terminal hydrophobic anchors into the ThT-reactive parallel β-structure, in which the local chemical environments of the C-terminal segments are different in different β-strands. This may account for the multiple HSQC peaks originating from the C-terminal segments (Figure 4).

It has been reported that Aβ exhibits ThT-reactive β-sheet-rich aggregates in the presence of sodium dodecyl sulfate (SDS) at submicellar concentrations [39, 40]. Under these conditions, all the amide peaks of Aβ(1–40) disappeared from the ^{1}H-^{15}N HSQC spectrum because of the formation of large aggregates, except for those from the C-terminal residues that should still be mobile in this assembly state. On the basis of the NMR data obtained using paramagnetic probes, the C-terminal segment of Aβ(1–40) bound to SDS micelles has shown to be exposed to aqueous environment, exhibiting higher mobility [41]. Taking into account these data in conjunction with our present data, we suggest that different β-like structures of Aβ(1–40) are induced by GM1 aqueous micelles and submicellar concentrations of SDS.

Lyso-GM1 micelles could not induce the formation of the ThT-reactive β-structure of Aβ(1–40) although the micelle-interacting modes of Aβ(1–40) are almost identical between GM1 and lyso-GM1 micelles under ganglioside-excess conditions [15]. By inspection of the dynamic light scattering data on an assumption of their globular shapes, the diameters of GM1 and lyso-GM1 micelles have been estimated as 12 nm and 8 nm, respectively. It is plausible that the sizes and curvatures of the gangliosidic micelles are determining factors for the number of Aβ molecules that can be accommodated on their hydrophilic/hydrophobic interface and the occurrence of Aβ-Aβ interactions coupled with ThT-reactive β-structure formation. Indeed, GM1 clusters with flatter curvature such as GM1-containing unilamellar vesicles induce enhanced Aβ fibrillogenesis [5] in comparison with GM1 micelles. Lipid composition can also be a determining factor for assembly states of GM1 molecules and their interaction with Aβ. Most importantly, there is growing evidence that cholesterol and sphingomyelin contribute to GM1 assembly and thereby influence Aβ deposition promoted by its cluster [8, 18, 42, 43]. Elucidation of the structural basis of these molecular events is an important subject for the forthcoming stage of the research.

In conclusion, in the present study, we firstly identified and characterized the ThT-reactive β-structure of Aβ(1–40) promoted on GM1 micelles. Our findings offer structural insights into the mechanisms underlying the α-to-β conformational transition of Aβ on GM1 clusters, which is associated with the nucleation process in the Aβ aggregation.

Abbreviations

Aβ : Amyloid β
AD: Alzheimer's disease
CD: Circular dichroism
GST: Glutathione *S*-transferase
His_6-Ub: Hexahistidine-tagged ubiquitin
HSQC: Heteronuclear single-quantum correlation
IPTG: Isopropyl-β-$_D$-thiogalactopyranoside
NMR: Nuclear magnetic resonance
SDS: Sodium dodecyl sulfate
ThT: Thioflavin T
VUV: Vacuum-ultraviolet
YUH-1: Yeast ubiquitin hydrolase-1.

Acknowledgments

The authors wish to acknowledge Dr. Yoshiki Yamaguchi (RIKEN) for his useful discussions on the NMR analyses. This work was supported in part by the Nanotechnology Network Project and Grants-in-Aid for Scientific Research (nos. 20023033 and 20107004) from the Ministry of Education, Culture, Sports, Science, and Technology of Japan, the CREST project from the Japan Science and Technology Agency, and the Research Funding for Longevity Sciences (22–14) from National Center for Geriatrics and Gerontology, Japan. M. Yagi- Utsumi is a recipient of a Japan Society for the Promotion of Science Research Fellowship for Young Scientists.

References

[1] F. Chiti and C. M. Dobson, "Protein misfolding, functional amyloid, and human disease," *Annual Review of Biochemistry*, vol. 75, pp. 333–366, 2006.

[2] G. B. Irvine, O. M. El-Agnaf, G. M. Shankar, and D. M. Walsh, "Protein aggregation in the brain: the molecular basis for Alzheimer's and Parkinson's diseases," *Molecular Medicine*, vol. 14, no. 7-8, pp. 451–464, 2008.

[3] J. A. Hardy and G. A. Higgins, "Alzheimer's disease: the amyloid cascade hypothesis," *Science*, vol. 256, no. 5054, pp. 184–185, 1992.

[4] A. T. Petkova, W. M. Yau, and R. Tycko, "Experimental constraints on quaternary structure in Alzheimer's β-amyloid fibrils," *Biochemistry*, vol. 45, no. 2, pp. 498–512, 2006.

[5] K. Matsuzaki, K. Kato, and K. Yanagisawa, "Aβ polymerization through interaction with membrane gangliosides," *Biochimica et Biophysica Acta*, vol. 1801, no. 8, pp. 868–877, 2010.

[6] T. Ariga, M. P. McDonald, and R. K. Yu, "Role of ganglioside metabolism in the pathogenesis of Alzheimer's disease—a review," *Journal of Lipid Research*, vol. 49, no. 6, pp. 1157–1175, 2008.

[7] K. Matsuzaki, "Physicochemical interactions of amyloid β-peptide with lipid bilayers," *Biochimica et Biophysica Acta*, vol. 1768, no. 8, pp. 1935–1942, 2007.

[8] N. Yamamoto, T. Matsubara, T. Sato, and K. Yanagisawa, "Age-dependent high-density clustering of GM1 ganglioside

at presynaptic neuritic terminals promotes amyloid β-protein fibrillogenesis," *Biochimica et Biophysica Acta*, vol. 1778, no. 12, pp. 2717–2726, 2008.

[9] N. Yamamoto, Y. Hirabayashi, M. Amari et al., "Assembly of hereditary amyloid β-protein variants in the presence of favorable gangliosides," *FEBS Letters*, vol. 579, no. 10, pp. 2185–2190, 2005.

[10] S. Kumar-Singh, P. Cras, R. Wang et al., "Dense-core senile plaques in the Flemish variant of Alzheimer's disease are vasocentric," *American Journal of Pathology*, vol. 161, no. 2, pp. 507–520, 2002.

[11] C. L. Schengrund, "Lipid rafts: keys to neurodegeneration," *Brain Research Bulletin*, vol. 82, no. 1-2, pp. 7–17, 2010.

[12] J. Fantini and N. Yahi, "Molecular insights into amyloid regulation by membrane cholesterol and sphingolipids: common mechanisms in neurodegenerative diseases," *Expert Reviews in Molecular Medicine*, vol. 12, p. e27, 2010.

[13] M. Vey, S. Pilkuhn, H. Wille et al., "Subcellular colocalization of the cellular and scrapie prion proteins in caveolae-like membranous domains," *Proceedings of the National Academy of Sciences of the United States of America*, vol. 93, no. 25, pp. 14945–14949, 1996.

[14] T. Miura, M. Yoda, N. Takaku, T. Hirose, and H. Takeuchi, "Clustered negative charges on the lipid membrane surface induce β-sheet formation of prion protein fragment 106-126," *Biochemistry*, vol. 46, no. 41, pp. 11589–11597, 2007.

[15] M. Utsumi, Y. Yamaguchi, H. Sasakawa, N. Yamamoto, K. Yanagisawa, and K. Kato, "Up-and-down topological mode of amyloid β-peptide lying on hydrophilic/hydrophobic interface of ganglioside clusters," *Glycoconjugate Journal*, vol. 26, no. 8, pp. 999–1006, 2009.

[16] M. Yagi-Utsumi, T. Kameda, Y. Yamaguchi, and K. Kato, "NMR characterization of the interactions between lyso-GM1 aqueous micelles and amyloid β," *FEBS Letters*, vol. 584, no. 4, pp. 831–836, 2010.

[17] I. Mikhalyov, A. Olofsson, G. Gröbner, and L. B.Å. Johansson, "Designed fluorescent probes reveal interactions between amyloid-β(1-40) peptides and GM1 gangliosides in micelles and lipid vesicles," *Biophysical Journal*, vol. 99, no. 5, pp. 1510–1519, 2010.

[18] A. Kakio, S. I. Nishimoto, K. Yanagisawa, Y. Kozutsumi, and K. Matsuzaki, "Cholesterol-dependent formation of GM1 ganglioside-bound amyloid β-Protein, an endogenous seed for Alzheimer amyloid," *Journal of Biological Chemistry*, vol. 276, no. 27, pp. 24985–24990, 2001.

[19] A. Kakio, S. I. Nishimoto, K. Yanagisawa, Y. Kozutsumi, and K. Matsuzaki, "Interactions of amyloid β-protein with various gangliosides in raft-like membranes: importance of GM1 ganglioside-bound form as an endogenous seed for Alzheimer amyloid," *Biochemistry*, vol. 41, no. 23, pp. 7385–7390, 2002.

[20] H. Naiki and F. Gejyo, "Kinetic analysis of amyloid fibril formation," *Methods in Enzymology*, vol. 309, pp. 305–318, 1999.

[21] N. Ojima, K. Sakai, K. Matsuo et al., "Vacuum-ultraviolet circular dichroism spectrophotometer using synchrotron radiation: optical system and on-line performance," *Chemistry Letters*, no. 6, pp. 522–523, 2001.

[22] K. Matsuo, K. Sakai, Y. Matsushima, T. Fukuyama, and K. Gekko, "Optical cell with a temperature-control unit for a vacuum-ultraviolet circular dichroism spectrophotometer," *Analytical Sciences*, vol. 19, no. 1, pp. 129–132, 2003.

[23] N. Sreerama and R. W. Woody, "Estimation of protein secondary structure from circular dichroism spectra: comparison of CONTIN, SELCON, and CDSSTR methods with an expanded reference set," *Analytical Biochemistry*, vol. 287, no. 2, pp. 252–260, 2000.

[24] K. Matsuo, R. Yonehara, and K. Gekko, "Improved estimation of the secondary structures of proteins by vacuum-ultraviolet circular dichroism spectroscopy," *Journal of Biochemistry*, vol. 138, no. 1, pp. 79–88, 2005.

[25] K. Matsuo, R. Yonehara, and K. Gekko, "Secondary-structure analysis of proteins by vacuum-ultraviolet circular dichroism spectroscopy," *Journal of Biochemistry*, vol. 135, no. 3, pp. 405–411, 2004.

[26] W. Kabsch and C. Sander, "Dictionary of protein secondary structure: pattern recognition of hydrogen-bonded and geometrical features," *Biopolymers*, vol. 22, no. 12, pp. 2577–2637, 1983.

[27] K. Matsuo, H. Watanabe, and K. Gekko, "Improved sequence-based prediction of protein secondary structures by combining vacuum-ultraviolet circular dichroism spectroscopy with neural network," *Proteins*, vol. 73, no. 1, pp. 104–112, 2008.

[28] B. A. Wallace and R. W. Janes, "Synchrotron radiation circular dichroism spectroscopy of proteins: secondary structure, fold recognition and structural genomics," *Current Opinion in Chemical Biology*, vol. 5, no. 5, pp. 567–571, 2001.

[29] G. R. Jones and D. T. Clarke, "Applications of extended ultra-violet circular dichroism spectroscopy in biology and medicine," *Faraday Discussions*, vol. 126, pp. 223–236, 2004.

[30] M. P. Williamson, YU. Suzuki, N. T. Bourne, and T. Asakura, "Binding of amyloid β-peptide to ganglioside micelles is dependent on histidine-13," *Biochemical Journal*, vol. 397, no. 3, pp. 483–490, 2006.

[31] L. P. Choo-Smith and W. K. Surewicz, "The interaction between Alzheimer amyloid β(1-40) peptide and ganglioside G(M1)-containing membranes," *FEBS Letters*, vol. 402, no. 2-3, pp. 95–98, 1997.

[32] J. McLaurin and A. Chakrabartty, "Membrane disruption by Alzheimer β-amyloid peptides mediated through specific binding to either phospholipids or gangliosides. Implications for neurotoxicity," *Journal of Biological Chemistry*, vol. 271, no. 43, pp. 26482–26489, 1996.

[33] M. R. H. Krebs, E. H. C. Bromley, and A. M. Donald, "The binding of thioflavin-T to amyloid fibrils: localisation and implications," *Journal of Structural Biology*, vol. 149, no. 1, pp. 30–37, 2005.

[34] C. Rodríguez-Rodríguez, A. Rimola, L. Rodríguez-Santiago et al., "Crystal structure of thioflavin-T and its binding to amyloid fibrils: insights at the molecular level," *Chemical Communications*, vol. 46, no. 7, pp. 1156–1158, 2010.

[35] C. Wu, Z. Wang, H. Lei, Y. Duan, M. T. Bowers, and J. E. Shea, "The binding of thioflavin T and its neutral analog BTA-1 to protofibrils of the Alzheimer's disease $A\beta_{16-22}$ peptide probed by molecular dynamics simulations," *Journal of Molecular Biology*, vol. 384, no. 3, pp. 718–729, 2008.

[36] S. Chimon, M. A. Shaibat, C. R. Jones, D. C. Calero, B. Aizezi, and Y. Ishii, "Evidence of fibril-like β-sheet structures in a neurotoxic amyloid intermediate of Alzheimer's β-amyloid," *Nature Structural and Molecular Biology*, vol. 14, no. 12, pp. 1157–1164, 2007.

[37] R. Šachl, I. Mikhalyov, M. Hof, and L. B. A. Johansson, "A comparative study on ganglioside micelles using electronic energy transfer, fluorescence correlation spectroscopy and light scattering techniques," *Physical Chemistry Chemical Physics*, vol. 11, no. 21, pp. 4335–4343, 2009.

[38] R. Tycko, "Progress towards a molecular-level structural understanding of amyloid fibrils," *Current Opinion in Structural Biology*, vol. 14, no. 1, pp. 96–103, 2004.

[39] A. Wahlström, L. Hugonin, A. Perálvarez-Marín, J. Jarvet, and A. Gräslund, "Secondary structure conversions of Alzheimer's Aβ(1-40) peptide induced by membrane-mimicking detergents," *FEBS Journal*, vol. 275, no. 20, pp. 5117–5128, 2008.

[40] D. J. Tew, S. P. Bottomley, D. P. Smith et al., "Stabilization of neurotoxic soluble β-sheet-rich conformations of the Alzheimer's disease amyloid-β peptide," *Biophysical Journal*, vol. 94, no. 7, pp. 2752–2766, 2008.

[41] J. Jarvet, J. Danielsson, P. Damberg, M. Oleszczuk, and A. Gräslund, "Positioning of the Alzheimer Aβ(1-40) peptide in SDS micelles using NMR and paramagnetic probes," *Journal of Biomolecular NMR*, vol. 39, no. 1, pp. 63–72, 2007.

[42] Y. Mao, Z. Shang, Y. Imai et al., "Surface-induced phase separation of a sphingomyelin/cholesterol/ganglioside GM1-planar bilayer on mica surfaces and microdomain molecular conformation that accelerates Aβ oligomerization," *Biochimica et Biophysica Acta*, vol. 1798, no. 6, pp. 1090–1099, 2010.

[43] A. Ferraretto, M. Pitto, P. Palestini, and M. Masserini, "Lipid domains in the membrane: thermotropic properties of sphingomyelin vesicles containing GM1 ganglioside and cholesterol," *Biochemistry*, vol. 36, no. 30, pp. 9232–9236, 1997.